

Three-dimensional printed cardiac fistulae: a case series

Nicholas Aroney^{1,2*}, Ryan Markham^{1,2}, Anthony Putrino^{1,2}, James Crowhurst^{1,2}, Douglas Wall^{1,2}, Gregory Scalia^{1,2}, and Darren Walters^{1,2}

¹The Prince Charles Hospital, Queensland, Australia; and ²The University of Queensland, Queensland, Australia

Received 26 October 2018; accepted 7 April 2019; online publish-ahead-of-print 4 May 2019

Background

Three-dimensional (3D) printing of cardiac fistulae allows for immediate understanding of their complex courses and anatomical relations. Models can be used to improve patient understanding, enhance the consenting process, facilitate communication between multidisciplinary staff at heart team meetings, and help plan surgical or percutaneous interventions.

Case summary

We report four cases where 3D printed models were used as an adjunct with traditional measures in treating patients with complex cardiac fistulae.

Discussion

In our cases, overall patient understanding was improved, staff at heart team meetings were more aware of anatomical anomalies and perioperatively planning saw adjustments made that may have ultimately benefited patient outcome. Our cases highlight the additional benefit that 3D printed models can play when treating patients with complex cardiac fistulae.

Keywords

Fistula • Congenital • 3D printing • Case report

Learning points

- Cardiac fistulae can have a complex anatomical course and relations making treatment decisions difficult.
- Three-dimensional printing can have an adjunctive benefit in demonstrating fistulae course and anatomical relations.
- Three-dimensional printed models are useful in aiding with patient education, heart team meeting communication, and perioperative planning.

Introduction

Cardiac fistulae can cause angina, myocardial ischaemia, cardiomyopathy, and arrhythmia. With complex anatomy and an extensive array of communications, treatment options including surgical correction and percutaneous catheter-guided closure can be technically demanding. Angiography and computed tomography (CT)

angiography are the mainstay in diagnosis and planning therapy for cardiac fistulae.¹ However, understanding the three-dimensional (3D) course relative to adjacent structures is difficult with these traditional imaging modalities. Three-dimensional printed cardiac models allow for immediate scale visualization and tactile feedback of coronary fistulae and potentially enhance procedural and patient outcome.

* Corresponding author. Tel: +617 3139 4000, Email: Nicholas.aroney@gmail.com

Handling Editor: Tom de Potter

Peer-reviewers: Giulio Conte and Habib Khan

Compliance Editor: Mark Philip Cassar

Supplementary Material Editor: Peregrine Green

© The Author(s) 2019. Published by Oxford University Press on behalf of the European Society of Cardiology.

This is an Open Access article distributed under the terms of the Creative Commons Attribution Non-Commercial License (<http://creativecommons.org/licenses/by-nc/4.0/>), which permits non-commercial re-use, distribution, and reproduction in any medium, provided the original work is properly cited. For commercial re-use, please contact journals.permissions@oup.com

Three-dimensional printing is emerging as a useful adjunct in planning cardiac fistulae intervention.² Furthermore, enhanced understanding aids with patient education, consent, heart team communication, and perioperative planning. We demonstrate four cases where 3D printed cardiac models provided an adjunctive benefit in planning procedures, consenting patients, and guiding therapy.

Timeline

scale representation of the defect. The model demonstrated the shape and size of the fistula in a 1:1 ratio. The model was used preoperatively in assessing size, positioning, and selecting the type of closure device. Following analysis of the model, the initial decision to use a circular closure device was changed to an Amplatzer Vascular plug III, which was more representative of the fistula's shape and size (Figure 1C). The procedure was performed under transoesophageal echocardiographic and fluoroscopic guidance. A 14 mm × 5 mm vas-

Presentation	Investigation	Pre-procedure	Post-procedure	Follow-up
Patient 1 • Diastolic murmur	TTE • Dilated LV with a RCA-RA fistula	<ul style="list-style-type: none"> • Catheterization QP:QS of 3:1 • Cardiac CT and TOE • 3D model printed • Patient consented with 3D model • Vascular plug sized using CT and 3D model 	<ul style="list-style-type: none"> • Procedural success • Discharged Day 2 	Follow-up at 1 year <ul style="list-style-type: none"> • Asymptomatic • TTE: Device well seated, no residual shunt
Patient 2 • Angina and recurrent heart failure	Cardiac CT • LAD-PA fistula	<ul style="list-style-type: none"> • 3D model printed • Patient consented with 3D model • Course and size of the fistula assessed on the model • Planned for retrograde access and occlusion with coiling 	<ul style="list-style-type: none"> • Procedural success • Resolution of angina 	Follow-up at 1 year <ul style="list-style-type: none"> • Improved angina • No further heart failure hospitalizations • Catheterization demonstrating occluded fistula
Patient 3 • Fever and <i>Streptococcus anginosus</i> bacteraemia	TTE • Markedly dilated RCA-LV fistula	<ul style="list-style-type: none"> • Cardiac CT and TOE • 3D model printed • Patient consented with model • Heart team meeting • Prolonged treatment for infective endocarditis • Planned for percutaneous closure 	<ul style="list-style-type: none"> • Operative success • Discharged with warfarin 	Follow-up at 1 month <ul style="list-style-type: none"> • Episode of atrial flutter, cardioverted • Remains asymptomatic
Patient 4 • Supraventricular tachycardia	TTE • LCx-coronary sinus fistula	<ul style="list-style-type: none"> • Cardiac CT • Heart team meeting • Decision for surgical repair and resection 	<ul style="list-style-type: none"> • Operative success • Discharged with warfarin 	Follow-up at 1 month <ul style="list-style-type: none"> • Episode of atrial flutter, cardioverted • Remains asymptomatic

CT, computed tomography; LAD, left anterior descending artery; LCx, left circumflex artery; LV, left ventricle; PA, pulmonary artery; RA, right atrium; RCA, right coronary artery; TOE, transoesophageal echocardiogram; TTE, transthoracic echocardiogram.

Case presentation

Patient 1

A 21-year-old female patient was referred for investigation of a murmur. Transthoracic echocardiogram (TTE) demonstrated a dilated left ventricle (LV) and a right coronary sinus to right atrial fistula, confirmed with transoesophageal echocardiography (TOE) (Figure 1A). Invasive haemodynamics revealed a significant left-to-right shunt with a Qp:Qs of 3:1 (Table 1). A cardiac CT scan was segmented and a 3D model of the fistula and adjacent structures was printed (Figure 1B and C).

The 3D printed model provided immediate understanding of the fistula's location, orientation to nearby coronary cusps, and a tactile

cular plug was positioned and deployed (Figure 1D). Intraoperative echocardiography confirmed successful delivery of the device (Figure 1E and F).

There was no residual shunt on a 12-month follow-up TTE. The patient remains asymptomatic.

Patient 2

A 69-year-old male patient presented with recurrent angina and heart failure. Transthoracic echocardiogram demonstrated a dilated cardiomyopathy with an ejection fraction of 30%. A CT coronary angiogram revealed a large left anterior descending artery (LAD) to pulmonary artery (PA) fistula (Figure 2A). Coronary angiography confirmed the large fistulae (Figure 2B and C) which may have been

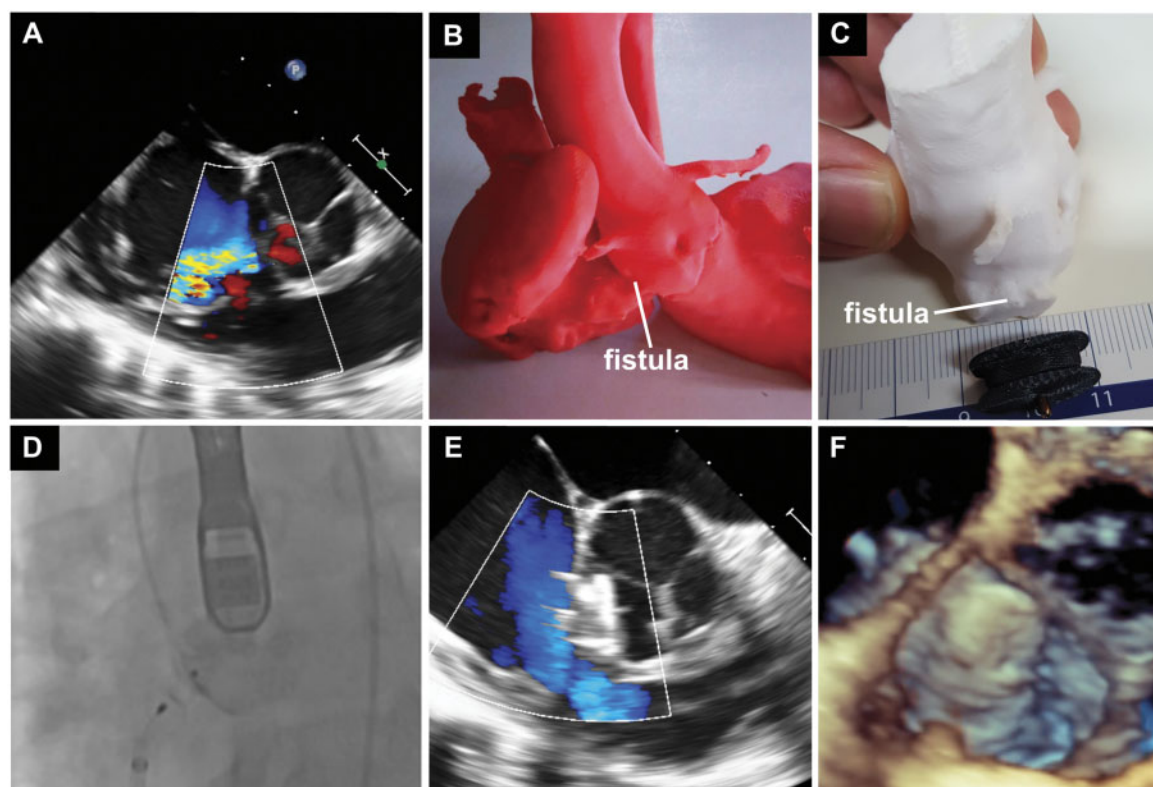


Figure 1 (A) TOE short axis at the aortic root demonstrating the fistula with colour-flow Doppler. (B) Three-dimensional printed model highlighting the position of the fistula between the right coronary cusp and right atrium, the right ventricle has been removed. (C) Three-dimensional model of the aortic root with the fistula sized next to an Amplatzer Vascular Plug III. (D) Fluoroscopic view confirming successful vascular plug implantation. (E) TOE short axis at the aortic root with colour-flow Doppler confirming obliteration of the fistula. (F) Three-dimensional TOE demonstrating successful implantation of the Amplatzer Vascular Plug III.

impacting on his symptoms via steal and contributing to his cardiomyopathy.

A 3D model of the relevant anatomy was printed (Figure 2D). On review of the model, given the size and the acute angle that the fistula took from the LAD, a percutaneous retrograde approach was planned.

The fistula was initially accessed antegrade with a 6-Fr Judkins Right (JR) 4 guide catheter. Following this, retrograde access via the left PA was obtained via the femoral vein using a courmand catheter upsized to an 8-Fr JR4. The fistula was successfully wired and a 6-Fr *GuideLiner*[™] (Vascular Solutions Inc., Minneapolis, MN, USA) was advanced retrograde into the fistula. Two 8 mm × 13.5 mm *Amplatzer*[™] (St. Jude Medical, St Paul, MN, USA) Vascular Plug IV devices were deployed (Figure 2E). A small amount of residual flow was noted at the end of the case.

On discharge, the patient noted an improvement in his symptoms.

Follow-up angiography at 1-year demonstrated successful occlusion of the fistula (Figure 2F).

Patient 3

A 25-year-old female patient presented with fevers and *Streptococcus anginosus* bacteraemia. Transthoracic echocardiogram

Table 1 Right heart catheterization

	Pressures (mmHg)	Saturations (%)
Inferior vena cava		64
Superior vena cava		65
Right atrium	7	84
Right ventricle	32/7	86
Main pulmonary artery	31/10/21	85
Pulmonary capillary wedge 11		
Ascending aorta		95

revealed a markedly dilated right coronary artery (RCA) with a fistula entering the basal inferior LV with turbulent Doppler flow across the mitral valve (MV) (Figure 3A). Transoesophageal echocardiography confirmed the dilated RCA (Figure 3B and D) and revealed a strand-like echodensity associated with the posterior MV leaflet tip, consistent with infective endocarditis. The patient was treated for infective endocarditis with a prolonged course of intravenous antibiotics.

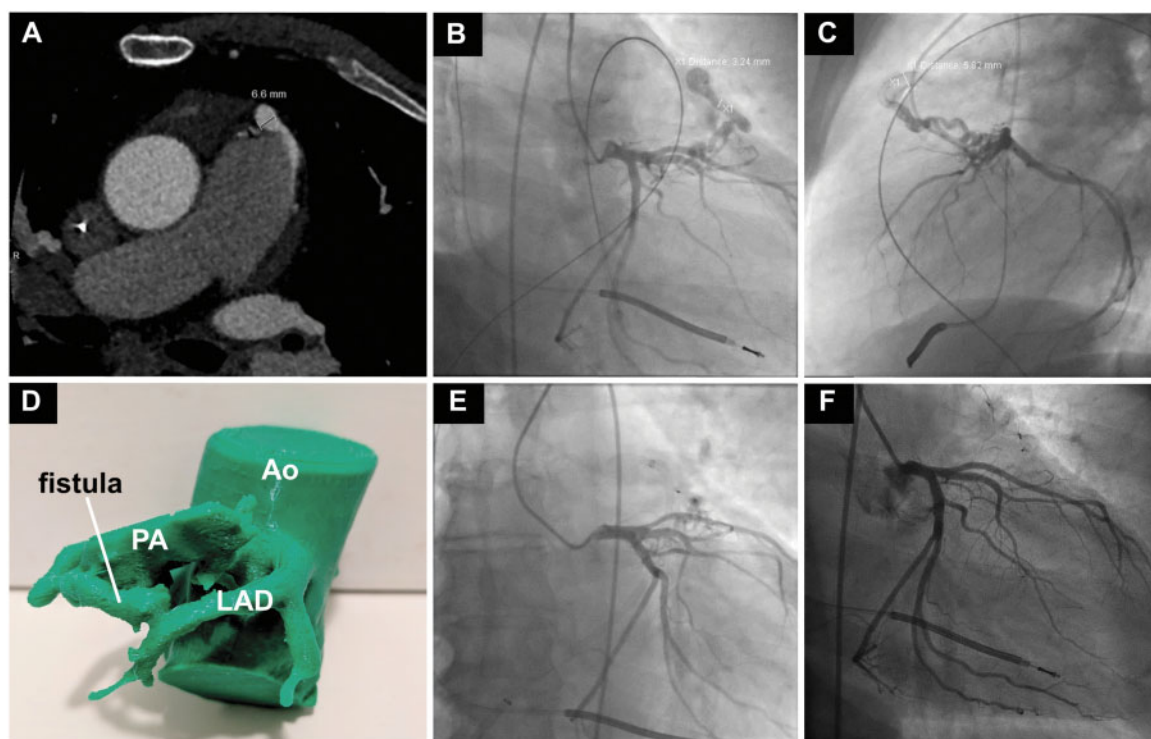


Figure 2 (A) Cardiac computed tomography demonstrating the left anterior descending artery to pulmonary artery fistula size and location. (B and C) Pre-procedural planning angiogram highlighting the complex course of the fistula. (D) Annotated three-dimensional printed model of the aortic root, left anterior descending artery, pulmonary artery, and fistula. (E) Procedural angiogram with retrograde delivery of two vascular plugs. (F) Angiogram at 1-year follow-up confirming successful closure of the fistula.

The case was presented at a multidisciplinary heart team meeting. Given the significant rupture risk that her dilated RCA-LV fistulae posed, the decision was made for elective percutaneous closure 6 months after clearance from infection. A cardiac CT was performed (Figure 3C) and a 3D model of the coronary arteries and LV was printed (Figure 3E and F). The model clearly demonstrated the dilated RCA fistulating with the LV, with an attractive distal target for percutaneous closure (Figure 3E and F). On presentation to the patient, the model clearly highlighted the anomalous artery, improving the understanding of the proposed procedure and overall informed consenting process.

The patient is currently completing a prolonged 6-month course of antibiotics prior to planned percutaneous intervention.

Patient 4

A 55-year-old female patient presented with palpitations. A 12-lead electrocardiograph showed a narrow-complex supraventricular tachycardia. A transoesophageal echocardiogram (TOE) demonstrated normal left ventricular size and function and a severely dilated coronary sinus, 50 mm × 50 mm (Figure 4A). Cardiac magnetic resonance imaging (MRI) confirmed the finding of a massively dilated coronary sinus (Figure 4B). A cardiac CT highlighted the marked dilatation and tortuosity of the left main and circumflex arteries and identified the two fistulous connections between the distal circumflex artery and the coronary sinus (Figure 4C). Dilated pulmonary arteries

and veins suggested a significant left-to-right shunt. Invasive catheterization and haemodynamics confirmed a significant shunt with a Qp:Qs of 1.8:1 (Figure 4D).

A 3D model was printed and presented at a heart team meeting (Figure 4E), this facilitated discussion between multidisciplinary staff. The 3D model provided immediate understanding and highlighted the complex course and fistulous connections. The model was particularly useful in assessing the anatomical size and location of the anatomy prior to intraoperative assessment which sees the heart and anatomy deflated whilst on a cardiopulmonary bypass pump. The heart team determined that the dilated coronary artery and coronary sinus posed a significant thrombosis and dissection risk. The model allowed for a tactile, scale representation of the anatomy and was used in the planning stages prior to surgery. Surgical resection and repair of the circumflex and coronary sinus was undertaken (Figure 4F).

The patient was discharged on warfarin to prevent thrombosis of the circumflex artery. She presented to the hospital 1 month following the procedure with atrial flutter. She was cardioverted and has remained asymptomatic since.

Discussion

Complex cardiac surgical and interventional procedures have traditionally used volume rendered MRI and CT for preprocedural

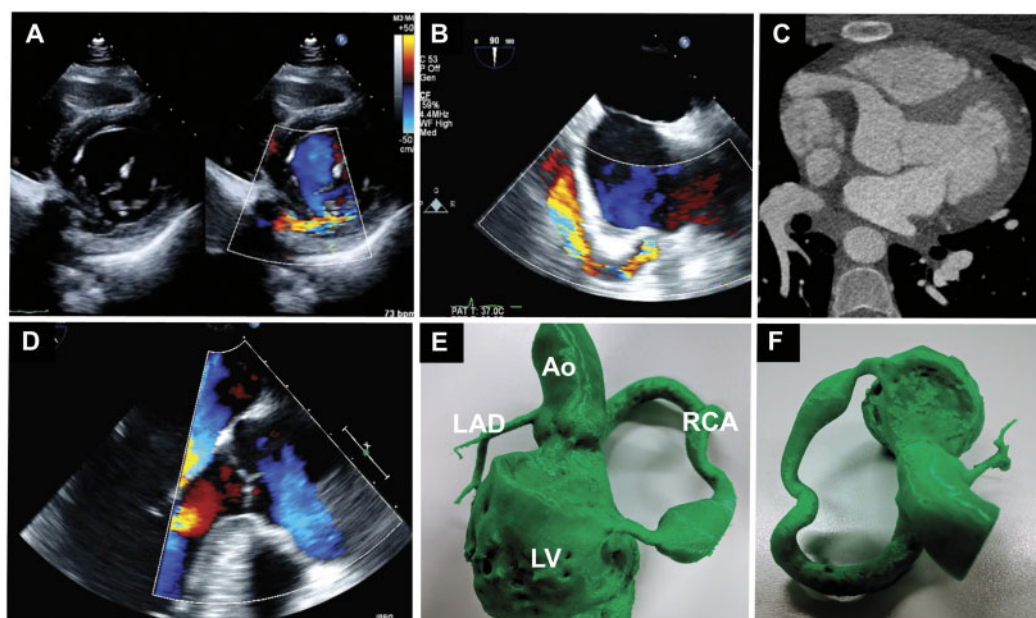


Figure 3 (A) Transthoracic echocardiogram short axis at the mitral valve demonstrating turbulent flow of the fistula with colour-flow Doppler. (B) TOE bicaval view highlighting the fistula size and location with colour-flow Doppler. (C) Cardiac computed tomography axial view demonstrating a severely dilated right coronary artery. (D) TOE long axis view with colour-flow Doppler highlighting the enlarged right coronary artery ostium. (E and F) Annotated three-dimensional printed model clearly depicting the size, course, and anastomosis of the fistulous right coronary artery.

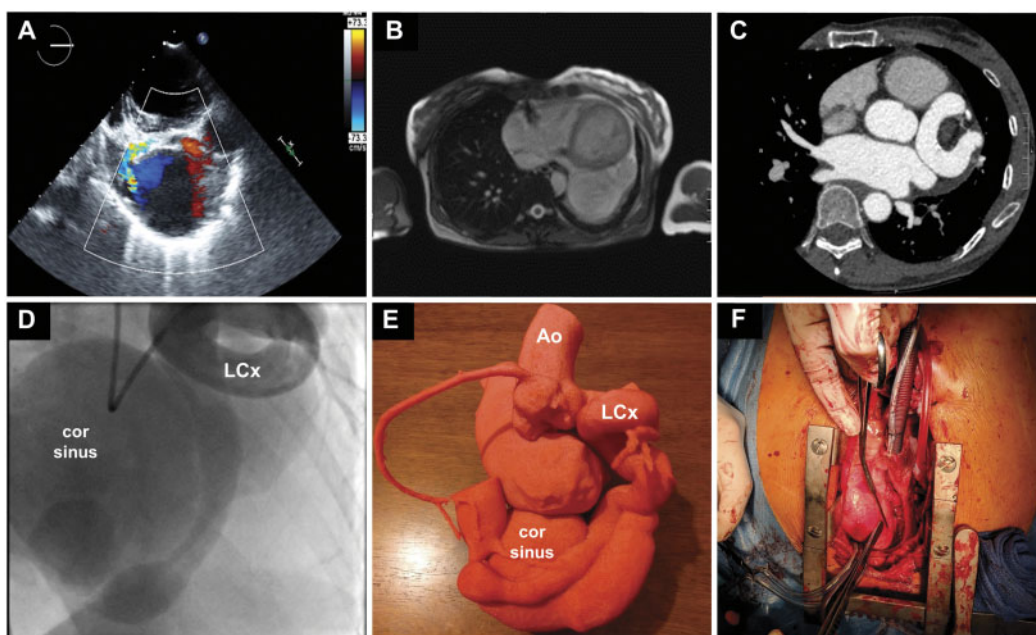


Figure 4 (A) TOE demonstrating the dilated coronary sinus with colour-flow Doppler. (B) Cardiac magnetic resonance imaging axial view highlighting the coronary sinus size. (C) Cardiac computed tomography axial view demonstrating the enlarged and tortuous left circumflex artery. (D) Invasive coronary angiography of the left coronary artery system demonstrating contrast filling of the coronary sinus. (E) Annotated three-dimensional printed model showing the size, course, and anastomosis of the fistulous left circumflex artery. (F) Intraoperative photo of the surgeons view after sternotomy.

visualization. More recently, 3D printing of complex cardiac anatomy is demonstrating adjunctive benefits in patient consent, heart team communication, and periprocedural planning.^{2–4} By isolating relevant anatomy in the segmentation process, 3D printed models allow for simplified interpretation and immediate understanding of complex anatomy.

The 3D segmentation process is becoming more streamlined with the use of semi-automated analysis software.⁵ With advances in 3D printer technology, printing is becoming less expensive and more accessible, giving medical departments access to desktop sized printers capable of detailed resolutions. However, one of the limitations of these less expensive models is that they use a rigid material, not optimal in mimicking the elasticity of biological tissue.⁵

In our case series, 3D printed models were used to enhance the consenting process. Three-dimensional models allowed for patient-specific and scale representation of their anatomy. This eventuated in a more thorough understanding of the underlying pathology and proposed treatment and ultimately a more informed consent.

The heart team meeting is vital in the management of the structurally complex cardiac patient. Three-dimensional printed models were used in a number of our meetings allowing all attendees to have a sound understanding of the relevant anatomy, facilitating clear communication between disciplines.

Haptic feedback and pre-procedural 3D visualization allowed for enhanced perioperative planning. Benefits were noted in the understanding of anatomical relationships and decisions with fistulae access as well as equipment choice. Using 3D models as an adjunctive measure perioperatively may improve procedural times, reduce complications, and increase the likelihood of procedural success.

Finally, after 3D printed models have served their initial clinical purposes, we have found additional benefit with using the models as tools to enhance medical education.

Supplementary material

Supplementary material is available at *European Heart Journal - Case Reports* online.

Slide sets: A fully edited slide set detailing this case and suitable for local presentation is available online as **Supplementary data**.

Consent: The author/s confirm that written consent for submission and publication of this case report including image(s) and associated text has been obtained from the patient in line with COPE guidance.

Conflict of interest: none declared.

References

1. Pursnani A, Jacobs JE, Saremi F, Levisman J, Makaryus AN, Capuñay C, Rogers IS, Wald C, Azmoon S, Stathopoulos IA, Srichai MB. Coronary CTA assessment of coronary anomalies. *J Cardiovasc Comput Tomogr* 2012;**6**:48–59.
2. Velasco Forte MN, Byrne N, Valverde Perez I, Bell A, Gómez-Ciriza G, Krasemann T, Sievert H, Simpson J, Pushparajah K, Razavi R, Qureshi S, Hussain T. 3D printed models in patients with coronary artery fistulae: anatomical assessment and interventional planning. *EuroIntervention* 2017;**13**:e1080–e1083.
3. Valverde I, Gomez G, Suarez-Mejias C, Hosseinpour AR, Hazekamp M, Roest A, Vazquez-Jimenez JF, El-Rassi I, Uribe S, Gomez-Cia T. 3D printed cardiovascular models for surgical planning in complex congenital heart diseases. *J Cardiovasc Magn Reson* 2015;**17**:196.
4. Marone EM, Rinaldi LF, Pietrabissa A, Argentero A. Effectiveness of 3D printed models in obtaining informed consent to complex aortic surgery. *J Cardiovasc Surg* 2018;**59**:488–489.
5. Garcia J, Yang Z, Mongrain R, Leask RL, Lachapelle K. 3D printing materials and their use in medical education: a review of current technology and trends for the future. *BMJ Simul Technol Enhanc Learn* 2018;**4**:27–40.